



Treball final de grau

GRAU DE MATEMÀTIQUES

Facultat de Matemàtiques
Universitat de Barcelona

**PARAMETERIZATION OF
INVARIANT MANIFOLDS: THE
LORENZ MANIFOLD**

Autor: Irene Roma Gimeno

Director: Dr. Alejandro Haro Provinciale
Realitzat a: Departament de
Matemàtica aplicada i anàlisi

Barcelona, June 27, 2016

Abstract

This work is composed of three different parts. First of all, a deep study of the Lorenz equations is done, beginning with its physical deduction, continuing with its dynamical properties and ending with the discussion of three typical properties of chaotic attractors (*Volume contraction*, *Local instability* and *global stability* and how they are illustrated by the Lorenz system. The second part is based on Taylor's method as a numerical integration method for the Lorenz differential equation system. The order of the expansion and the step size are the parameters to determine in order to have an error below a certain tolerance and a high computational efficiency. The last part is the one which gives the title to this project. Once we have a deep understanding of the dynamical system and a way to integrate it we can proceed to find an approximation for the invariant stable manifold using the parameterization method. A general theorem for the analytic case is first introduced and then the method is adapted to the Lorenz model, and hence obtaining a plot of this manifold.

Acknowledgments

I would like to thank professor Alejandro Haro for his time, patience and great advice. Without his support and help I would not have been able achieved this work. I also thank my parents, my sister Jana and my great friends Albert, Marta and Martí, since their support has been essential.

'Small changes can have large consequences' - E.Lorenz

Contents

1	Introduction	1
2	The Lorenz System	2
2.1	Physical deduction of the Lorenz equations	2
2.2	Dynamics of the equations	6
2.2.1	Fixed points and stability	6
2.2.2	Invariant Manifolds	9
2.3	Chaos	9
3	Numerical Integration	16
3.1	Intregation: Taylor method	16
3.2	Automatic differentiation	17
3.3	Step size control and degree	17
3.4	Example: The Lorenz System	19
4	The parameterization method for invariant manifolds	21
4.1	The parameterization method for flows	21
4.2	Manifolds associated to a fixed point of a vector field	22
4.3	Computation of Invariant Manifolds	22
4.3.1	The invariance Equation	23
4.3.2	The Cohomological Equations	24
4.3.3	The Normal Form Style	26
4.4	Example: Lorenz System	27
4.4.1	Maximum order and error	28
4.5	Results	30
5	Conclusions	33

1 Introduction

During the twentieth century there was a huge progress in the study of chaotic theory. Edward Lorenz was highly involved with the evolution of this theory and among his work there are some findings that especially stand out. For example, in 1960, he tried to duplicate a weather forecast he had previously done, but the result of his experiment was unexpected. Even though initial conditions were identical, the two forecast models diverged over few hundred of time steps and were no longer the same. He discovered that the computer had rounded off the two initial conditions differently and this difference had grown with each time step, so errors in initial conditions play an important role. This result forged one revolutionary concept: *small changes can have large consequences*, which is known as *the butterfly effect*.

The Lorenz system has been used in several fields, one of them being numerical weather prediction (NWP). Before the 1950s, weather forecasting was based on subjective interpretations of synoptic charts. Then, with the acquisition of experience from past weather situations, forecasts were improved by making use of historical analogs of the current weather situations. But this technique was limited because the observation of two very similar patterns has an extremely low probability. Weather forecasting made a big step with the first equation models based on dynamical principles and the beginning of NWP. From the fifties to today, NWP models have considerably improved. For example, Lorenz wrote an atmospheric model governed by 28 ODE and he observed a 4-day doubling time due to error propagation. He also realized that errors in small scales tend to amplify and thus becoming relevant in larger scales in a day or so, [Lor84]. Now there is a higher spatial resolution and a more accurate representation of physical processes, including parametric representations of unresolved processes (radiation, convection, diffusion, ...), [Bau15]. These progresses have been possible thanks to the advances in computer technology and science over the past decades which have remarkably improved forecast skills. A 3-day forecast has more than a 95% of accuracy and a 7-day forecast almost a 70%, [Wal06].

His work has also been important in the field of mathematics, on which this work will focus by studying qualitatively the Lorenz system. The qualitative study of a dynamical system starts considering its fixed points and periodic orbits and then considering the invariant manifolds associated with them. We focus the third and fourth sections on studying the computational aspects of numerical integration of differential equations and high order power series expansions of parameterizations for invariant manifolds of vector fields, in concrete the Lorenz system.

2 The Lorenz System

In this section we will begin with the physical deduction of the Lorenz equations inspired by one of the most important papers of E. Lorenz: *Deterministic Nonperiodic Flow* [Lor63]. In this paper he also gave some great ideas to prove that the Lorenz model can have a chaotic behavior and how we can numerically integrate the differential equations.

2.1 Physical deduction of the Lorenz equations

We are going to introduce an overview of the deduction of the Lorenz equations from the Navier-Stokes and thermal energy diffusion equation based on [Lor63] and [Hil00].

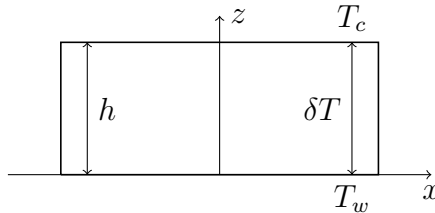


Figure 1: Fluid under Rayleigh-Bénard conditions. h is the height of the cell and $\delta T = T_w - T_c$.

The Lorenz model describes the motion of a fluid under Rayleigh-Bénard conditions i.e. an incompressible fluid contained in a cell which has a higher temperature at the bottom (T_w) and a lower temperature (T_c) at the top, as shown in figure 1. When the vertical temperature gradient becomes sufficiently large, a small packet of fluid moves upwards and experiences a net upward force (buoyancy force). If it is sufficiently strong, the packet will move more quickly than its temperature can drop, otherwise there will be no convection. This is regulated by one of the parameters of the equations, the Rayleigh number R .

Before starting with the equation deduction it is important to give physical meaning to the Rayleigh number. Considering that the packet finds itself displaced upwards by a small amount Δz , the temperature of the new region will be $T_n = T_w - \frac{\delta T}{h} \Delta z$ (figure 1). The introduction of an important parameter is now needed: the *thermal relaxation time* i.e. the time a small packet needs to reach the temperature of its surroundings. $t_r \frac{dT}{dt} = T_n - T_w$. Using the thermal diffusion equation (TDE) and an approximation of the Laplacian for small displacements:

$$\frac{dT}{dt} = D_T \nabla^2 T \approx -\frac{D_T \cdot \delta T \cdot \Delta z}{h^3} \rightarrow t_r = \frac{h^2}{D_T} \quad (2.1)$$

where D_T is the thermal diffusion coefficient. If t_r is bigger than the time of displacement (t_d) then there will be a convective state, otherwise the state will be

stable. To calculate t_d , the buoyant force ($F_B = -g \frac{d\rho}{dT} \Delta T$) and the fluid viscous force ($F_v \approx \mu \frac{v_z}{h^2}$) are set to be equal.

$$\left. \begin{aligned} \mu \frac{v_z}{h^2} &= \frac{\mu}{h^2} \frac{dz}{dt} \approx \frac{\mu}{h^2} \frac{h}{t_d} \\ -g \frac{d\rho}{dT} \Delta T &\approx -g \frac{d\rho}{dT} \delta T \end{aligned} \right\} \rightarrow t_d = \frac{\mu}{\alpha \rho_0 g h \delta T} \quad (2.2)$$

where $\alpha = -\frac{1}{\rho_0} \frac{d\rho}{dT}$ is the thermal expansion coefficient, ρ_0 the initial density and μ the fluid viscosity. So the critical parameter of convection, R , takes the form:

$$R = \frac{t_r}{t_d} = \frac{\alpha \rho_0 g h^3 \delta T}{D_T \mu} \quad (2.3)$$

At this point we can begin with the deduction of the Lorenz equations. It is possible to assume that the fluid flow is two dimensional and that it is incompressible, hence the density of an infinitesimal volume that moves with the flow velocity is constant. Therefore, only the x and z components are taken into account and the conservation law for the fluid density ($\frac{\partial \rho}{\partial t} = -\text{div}(\rho \vec{v})$) becomes $\text{div}(\vec{v}) = 0$. So the Navier-Stokes equations (NSE) and TDE are:

$$\rho \frac{\partial(v_x)}{\partial t} + \vec{v} \cdot \rho \nabla(v_x) = -\frac{\partial p}{\partial x} + \mu \nabla^2 v_x \quad (2.4)$$

$$\rho \frac{\partial(v_z)}{\partial t} + \vec{v} \cdot \rho \nabla(v_z) = -\rho g - \frac{\partial p}{\partial z} + \mu \nabla^2 v_z \quad (2.5)$$

$$\frac{\partial T}{\partial t} + \vec{v} \cdot \nabla T = D_T \nabla^2 T \quad (2.6)$$

where v_x and v_z are the horizontal and the vertical components of the velocity. In the vertical NSE, on the right hand side three different forces are considered: gravity, pressure gradient force and viscosity (per unit volume). And the left hand side represents the force per unit volume, that a packet receives with the Lagrangian point of view. This explanation is equivalent for the TDE. It is necessary to introduce some new variables and change some of the previous ones in order to obtain dimensionless NSE. The suggested changes are:

A new temperature function that describes the temperature deviation from its linear behavior:

$$\tau(x, z, t) = T(x, z, t) - T_w + \frac{z}{h} \delta T \quad (2.7)$$

The Taylor expansion of the density around T_w , truncated at second order, that takes into account its change with temperature.

$$\rho(T) = \rho(T_w) + \frac{\partial \rho}{\partial T} (T - T_w) = \rho_0 + \frac{\partial \rho}{\partial T} (\tau - \frac{z}{h} \delta T) \quad (2.8)$$

The Boussinesq approximation ignores the density variation when the force due to gravity is not involved, hence all the terms involving $\frac{\partial \rho}{\partial T}$ will be zero unless it also appears the gravity force.

An effective pressure (p_{ef}), that for non convecting states satisfies $\nabla p_{ef} = 0$.

$$p_{ef} = p + \rho_0 g z - z^2 \frac{\partial \rho}{\partial T} \frac{\partial T}{2h} \quad (2.9)$$

Finally, the time, space, temperature and pressure variables (t, x, z, τ, p_{eft}) are converted into dimensionless variables.

$$t' = \frac{D_T}{h^2} t, \quad x' = \frac{x}{h}, \quad z' = \frac{z}{h}, \quad \tau' = \frac{\tau}{\delta T}, \quad p' = \frac{p_{ef} h^2}{\mu D_T}$$

With all these changes the NSE and TDE become:

$$\frac{1}{\sigma} \left(\frac{\partial(v'_x)}{\partial t'} + \vec{v}' \cdot \rho \nabla'(v'_x) \right) = -\frac{\partial p'}{\partial x'} + \nabla'^2 v'_x \quad (2.10)$$

$$\frac{1}{\sigma} \left(\frac{\partial(v'_z)}{\partial t'} + \vec{v}' \cdot \rho \nabla'(v'_z) \right) = -\frac{\partial p'}{\partial z'} + R\tau' + \nabla'^2 v'_z \quad (2.11)$$

$$\frac{\delta \tau'}{\delta t'} + \vec{v}' \cdot \nabla \tau' - v'_z = \nabla'^2 \tau' \quad (2.12)$$

where the Prandtl number ($\sigma = \frac{\mu}{\rho_0 D_T}$) is the parameter of the Lorenz equations that measures the importance of viscosity in contrast to that of thermal diffusion.

In order to arrive to the common expression of the Lorenz equations a stream function related to the fluid velocity components is needed, which will then be substituted in equations 2.11, 2.10 and 2.12. This stream function can be defined because of the incompressibility of the fluid and the two dimensionality of the flow.

$$v_x = -\frac{\partial \Psi(x, z, t)}{\partial z} \quad v_z = \frac{\partial \Psi(x, z, t)}{\partial x}$$

and then,

$$\frac{1}{\sigma} \left(\frac{\partial^2 \Psi}{\partial t \partial x} - \frac{\partial \Psi}{\partial z} \frac{\partial^2 \Psi}{\partial x^2} + \frac{\partial \Psi}{\partial x} \frac{\partial^2 \Psi}{\partial x \partial z} \right) = -\frac{\partial p'}{\partial z} + R\tau + \nabla^2 \frac{\partial \Psi}{\partial x} \quad (2.13)$$

$$\frac{1}{\sigma} \left(\frac{\partial^2 \Psi}{\partial t \partial z} + \frac{\partial \Psi}{\partial z} \frac{\partial^2 \Psi}{\partial x \partial z} + \frac{\partial \Psi}{\partial x} \frac{\partial^2 \Psi}{\partial z \partial x} \right) = -\frac{\partial p'}{\partial x} - \nabla^2 \frac{\partial \Psi}{\partial z} \quad (2.14)$$

$$\frac{\partial \tau}{\partial t} - \frac{\partial \Psi}{\partial z} \frac{\partial \tau}{\partial x} + \frac{\partial \Psi}{\partial x} \frac{\partial \tau}{\partial z} - \frac{\partial \Psi}{\partial x} = \nabla^2 \tau \quad (2.15)$$

All the variables are dimensionless but we have simplified the notation. If we scale the dimension of the convective cell we can consider that the bottom is at $z = 0$ and the top at $z = 1$. In this points the variation of temperature τ is zero, because the temperatures are T_w and T_c respectively. The vertical velocity of the flow is zero, $v_z = 0$, and the variation of the horizontal velocity v_x with height is also null. This is because the shear forces are proportional to $\frac{\partial v_x}{\partial z}$ and at the top and the bottom surfaces we neglect them. Consistent with boundary conditions, and with the aim of simplifying the results, the suggested solutions are:

$$\Psi(x, z, t) = \Psi(t) \sin(\pi z) \sin(ax) \quad (2.16)$$

$$\tau(x, z, t) = T_1(t) \sin(\pi z) \cos(ax) - T_2(t) \sin(2\pi z) \quad (2.17)$$

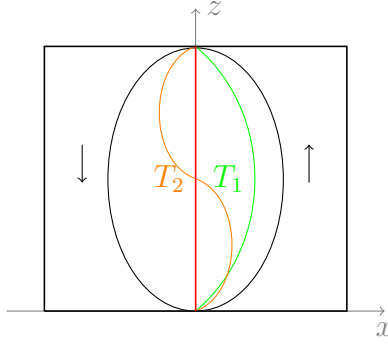


Figure 2: Convective cell. In green an approximation of the behavior of $T_1(x, z, t)$ and in orange an approximation of the behavior of $T_2(x, z, t)$.

The first term of the temperature deviation, $T_1(x, z, t)$, is the temperature difference between the upward and downward moving parts of a convective cell. The second term, $T_2(x, z, t)$, gives the deviation of the vertical temperature profile from linearity in the center, where it is considered zero (in red at figure 3). It is important to notice that the term $T_1(x, z, t)$ is proportional to the velocity v_z , and that the biggest gradients of $T_2(x, z, t)$ are located on the top and the bottom of the cell.

Finally, we use the suggested solutions in the equations 2.13, 2.14, 2.15 where some trigonometric terms involving $\sin(3\pi z)$ appear and are omitted. This implies that if the temperature difference between the top and the bottom of the convective cell becomes too large, this equations no longer provide a useful model of the dynamics of the fluid. The non linear system of differential equations for convection under Rayleigh-Bénard conditions, in other words, the Lorenz System is:

$$\begin{cases} \dot{X} = -\sigma X + \sigma Y \\ \dot{Y} = -XZ + rX - Y \\ \dot{Z} = XY - bZ \end{cases} \quad \text{with} \quad \begin{cases} X(t) = \frac{a\pi}{\sqrt{2(a^2+\pi^2)}} \Psi(t) \\ Y(t) = \frac{r\pi}{\sqrt{2}} T_1(t) \\ Z(t) = \pi r T_2(t) \end{cases} \quad (2.18)$$

where $r = R/C$ and b is a new parameter which solely depends on a . $C = (\pi^2 + a^2)^3/a^2$ is the critical value for R , so when it exceeds the value of C , convection will start. The physical interpretation of the variables which appear in the Lorenz equation is: x is proportional to the intensity of convective motion, y is proportional to the temperature between the raising (warm) and sinking (cool) fluid of a convective cell and z is proportional to the deviation of the vertical temperature profile from linearity.

2.2 Dynamics of the equations

In this section is given a general view of the dynamics of the Lorenz System.

$$\begin{cases} \dot{x} = -\sigma x + \sigma y \\ \dot{y} = -xz + rx - y \\ \dot{z} = xy - bz \end{cases} \quad (2.19)$$

Note 1. : during the discussion in some cases are used the most common values for $\sigma = 10$ and $b = 8/3$, also used by Lorenz, [Lor63]. The dynamic discussion then is done around the parameter r .

2.2.1 Fixed points and stability

Let us show that Lorenz equations exhibit the following symmetry: $s(x, y, z) = (-x, -y, z)$, $Ds \cdot F = F \circ s = F(s)$, by proving that $F(s(x, y, z)) = F(x, y, z)$.

Proof.

$$F(s(x, y, z)) = \begin{cases} -\dot{x} = -\sigma(-x) + \sigma(-y) \\ -\dot{y} = xz + r(-x) - (-y) \\ \dot{z} = (-x)(-y) - bz \end{cases} = \begin{cases} -\dot{x} = +\sigma x - \sigma y \\ -\dot{y} = xz - rx + y \\ \dot{z} = xy - bz \end{cases} = F(x, y, z)$$

□

Fixed points of a dynamical system $F(x) = \dot{x}$ are those which $F(x^*) = 0$. In the Lorenz system:

$$\begin{cases} -\sigma x + \sigma y = 0 \\ xz + rx - y = 0 \\ xy - bz = 0 \end{cases} \Rightarrow \begin{cases} x = y \\ x(-z + r - 1) = 0 \\ x = \pm\sqrt{zb} \end{cases}$$

$$x = 0 \rightarrow O = (0, 0, 0)$$

$$-z + r - 1 = 0 \rightarrow C_{\pm} = \left(\pm\sqrt{(r-1)b}, \pm\sqrt{(r-1)b}, r-1 \right)$$

Note 2. Notice that the origin is a fixed point for all values of $r > 0$ but C_{\pm} only for $r \geq 1$.

Here we can introduce an important concept, the omega limit set, which will be useful to characterize the famous Lorenz attractor.

Definition 2.2.1.1. We define the ω -limit set of a trajectory $x(t)$ to be all those points of the domain which are limits of a sequence of the form $x(t_n)$ for $t \rightarrow \infty$.

The stability of the fixed points is studied by calculating the eigenvalues of the $DF(x)$ matrix evaluated at the different fixed points.

$$DF(x^*) = \begin{pmatrix} -\sigma & \sigma & 0 \\ -z^* + r & -1 & -x^* \\ y^* & x^* & -b \end{pmatrix}$$

So we need to solve $A(F_i) - \lambda I = 0$ for $i = 1, 2, 3$.

$$\boxed{i = 1}$$

$$\det(A(r) - \lambda I) = \begin{vmatrix} -\sigma - \lambda & \sigma & 0 \\ r & -1 - \lambda & 0 \\ 0 & 0 & -b - \lambda \end{vmatrix} = 0$$

$$\rightarrow (b + \lambda)(\sigma(r - 1) + (1 + \sigma)\lambda + \lambda^2) = 0$$

$$\begin{cases} \lambda_2 = -b \in \mathbb{R} \\ \lambda_{3,1} = \frac{-1 - \sigma \pm \sqrt{(\sigma + 1)^2 - 4\sigma(1 - r)}}{2} \in \mathbb{R} \end{cases}$$

For $0 < r < 1$, $\lambda_{1,2,3} < 0 \rightarrow O$ is stable

For $r \geq 1$, $\lambda_{1,2} < 0$ and $\lambda_3 > 0 \rightarrow O$ is unstable

The notation of the eigenvalues tries to be consistent with section 4.

$$\boxed{i = 2, 3}$$

$$\det(A(C_{\pm}) - \lambda I) = \begin{vmatrix} -\sigma - \lambda & \sigma & 0 \\ 1 & -1 - \lambda & \mp \sqrt{(r - 1)b} \\ \pm \sqrt{(r - 1)b} & \pm \sqrt{(r - 1)b} & -b - \lambda \end{vmatrix} = 0$$

$$\rightarrow P(\lambda) = \lambda^3 + (\sigma + b + 1)\lambda^2 + b(r + \sigma)\lambda + 2b\sigma(r - 1) = 0$$

Since σ , b , and r are positive parameters, $P'(\lambda) > 0$ for all $\lambda \geq 0$. And for $\lambda = 0$, $P(0) > 0$, [Pei92]. So we conclude that at least one of the roots of the characteristic polynomial has to be real and negative, $\lambda_1 < 0$. For the other two roots we can consider two options: then can be both real and negative or they can be a complex conjugate pair. $\lambda_{2,3} = \alpha \pm i\beta$.

Depending on the sign of the real part of the complex numbers the stability of the fixed points will change.

For $\alpha < 0$, C_{\pm} will be stable. The stability boundary lies at $\alpha = 0$:

$$\begin{aligned} P(i\beta) &= (i\beta)^3 + (\sigma + b + 1)(i\beta)^2 + b(r + \sigma)(i\beta) + 2b\sigma(r - 1) \\ &= (2b\sigma(r - 1) - (b + \sigma + 1)\beta^2) + i(b(\sigma + r) - \beta^2)\beta = 0 \end{aligned}$$

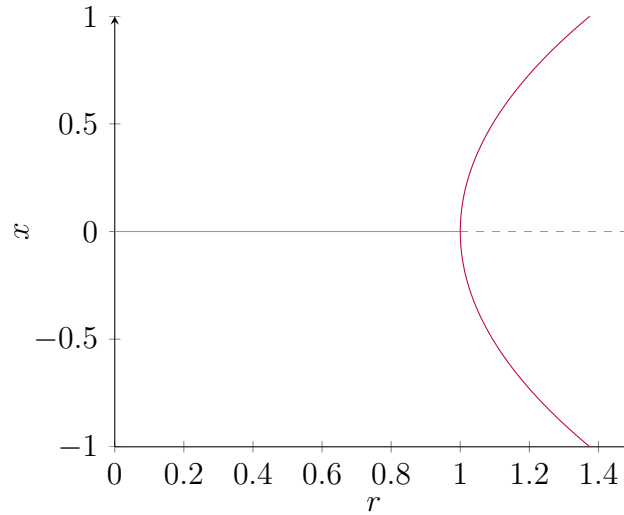
Solving the two equations for $r(\sigma, b)$,

$$\left. \begin{aligned} 2b(r - 1) - (b + \sigma + 1)\beta^2 &= 0 \\ b(\sigma + r) - \beta^2 &= 0 \end{aligned} \right\} \rightarrow r_H = \frac{\sigma(\sigma + b + 3)}{\sigma - b - 1}$$

For the current values of b and σ , $r_H \approx 24.74$. It is also observed that for $r_* \approx 24.06$ the chaotic attractor shown in figure 8 is observed numerically i.e. the choice of almost any initial condition in a neighborhood set results in a similar figure.

Summing up all this information:

- For $0 < r < 1$, the origin is the only fixed point and it is globally stable.
- For $r = 1$, a super critical pitchfork bifurcation occurs. So the stable fixed point r loses its stability and in its place appear to new fixed stable points C_{\pm} .



- For $1 < r < r_H$, C_{\pm} are stable fixed points and the origin remains as an unstable fixed point. If $r \leq r_*$ then there are chaotic orbits but not chaotic attractors and for $r \geq r_*$ there is a chaotic attractor coexisting with the attracting fixed points C_{\pm} .
- For $r = r_H$, a subcritical Hopf bifurcation occurs. So C_{\pm} lose their stability and the three fixed points become unstable. The chaotic attractor still exists.

2.2.2 Invariant Manifolds

For a fixed point x^* in a nonlinear system, the stable manifold of x^* , $\mathfrak{W}^s(x^*)$ is the set of initial conditions for which the solution $x(t)$ tends to x^* as $t \rightarrow \infty$, while the unstable manifold $\mathfrak{W}^u(x^*)$ is the set of initial conditions for which the solution $x(t)$ tends to x^* as $t \rightarrow -\infty$

The Stable Manifold Theorem states that if the eigenvalues of the linearized system (Df) have all real part different from zero then $\mathfrak{W}^s(x^*)$ and $\mathfrak{W}^u(x^*)$ exist and their dimension is the same as the stable and unstable subspaces generated by the eigenvectors, respectively.

The Lorenz System around the origin has one stable manifold of dimension two, two of the eigenvalues have negative real part, and one unstable manifold of dimension one, the remaining eigenvalue has positive real part. In section 4 we will give a parametrization of the stable manifold \mathfrak{W}^s .

2.3 Chaos

Definition 2.3.0.1. *The so called **Lorenz attractor** is the ω -limit set of an orbit $x(t)$ of the Lorenz system, with initial conditions $x(t_0) = x_0$.*

But, is the Lorenz attractor chaotic? This is not an easy question to be answered. It was affirmatively answered by Warwick Tucker in 2002, when he proved that the Lorenz attractor is a strange attractor, [Tuc02]. We want to illustrate its chaotic properties. There are three typical properties of chaotic attractors: *volume contraction*, *global stability* and *local instability*. So we will begin showing how they can be illustrated by the Lorenz attractor, [All96].

1. **Volume contraction:** The system is *dissipative* i.e. volumes in phase space contract under the flow.

Let $F(x) = \dot{x}$ be a dynamical system and $u(t) = \varphi_t(x_0)$. Consider then the volume of $u(t)$ defined by $V(t) = \text{vol}(u(t))$. Then the Liouville theorem we saw in the course of EDOs tells us that:

$$\frac{dV(t)}{dt} = \int_{u(t)} \text{div}F(x)dx \quad (2.20)$$

In our particular dynamical system, the Lorenz system:

$$\text{div}f = \frac{\delta\sigma(y-x)}{\delta x} + \frac{\delta(-xz+rx-y)}{\delta y} + \frac{\delta(xy-bz)}{\delta z} = -\sigma - 1 - b$$

which is constant. So $\frac{dV(t)}{dt} = \int_{u(t)} \text{div}F(x)dx = \int_{u(t)} (-\sigma - 1 - b)dx = -(\sigma + 1 + b)V$ and the evolution in volumes on the phase space is:

$$V(t) = V(0)e^{(-\sigma-1-b)t}$$

As $-\sigma - 1 - b < 0$ the evolution of volumes in the phase space is to shrink until a limiting set of zero volume.

2. **Global stability:** If there exists a trapping region around the origin then the orbits do not diverge to infinity and the system presents global stability.

Lemma 2.3.0.1. [All96] Let $\mathbf{u}(t) = (x(t), y(t), z(t))$ and let $E(\mathbf{u})$ be a smooth real-valued function with the property that $E(\mathbf{u}) \rightarrow \infty$ as $\|\mathbf{u}\| \rightarrow \infty$. Assume that there are constants $a_1, a_2, a_3 > 0$ and b_1, b_2, b_3, c such that $\forall x, y, z$:

$$\dot{E}(x, y, z) \leq -a_1x^2 - a_2y^2 - a_3z^2 + b_1x + b_2y + b_3z + c$$

Then there is a $B > 0$ such that every trajectory $\mathbf{u}(t)$ satisfies $|\mathbf{u}(t)| \leq B$ for all sufficiently large time t .

Taking $E(x, y, z) = \frac{1}{2}(x^2 + y^2 + (z - \sigma - r)^2)$, then $\dot{E}(x, y, z) = -\sigma x^2 - y^2 - bz^2 + b(\sigma + r)z$, which satisfies the lemma 2.3.0.1. All the trajectories stay bounded in some three-dimensional space.

3. **Local instability:** looking the trajectory of the Lorenz attractor in figure 8 we can think intuitively that it is chaotic but we don't have a rigorous proof of it. We should be able to affirm that the Lyapunov exponents are positive and that the attractor is not periodic. We will introduce some ideas that leads us to the conclusion that we have this conditions.

Definition 2.3.0.2. Let f be a smooth one-dimensional map of the real line \mathbb{R} . The **Lyapunov exponent** $h(x_1)$ of the orbit $\{x_1, x_2, x_3, \dots\}$ is defined as

$$h(x_1) = \lim_{n \rightarrow \infty} \frac{1}{n} [\ln |f'(x_1)| + \dots + \ln |f'(x_n)|]$$

if the limit exist. The **Lyapunov number** $L(x_1)$ is defined as:

$$L(x_1) = \lim_{n \rightarrow \infty} (|f'(x_1)| + \dots + |f'(x_n)|)^{1/n}$$

if the limit exists. So the relation between the two parameters is $\ln L(x_1) = h(x_1)$.

Definition 2.3.0.3. The **Lyapunov exponents** (respectively numbers) of a flow $\varphi_T(v)$ are defined to be the Lyapunov exponents (numbers) of the associated time-1 map.

The theory of Lyapunov exponents of a flow can be checked in [All96]. The Lyapunov exponents themselves quantify the degree of sensitivity with respect to the initial conditions. Let us explain how to calculate these exponents.

Let $F(x) = \dot{x}$ a dynamical system with initial conditions, $x(0) = x_0$, and $\varphi(t; x_0)$ its flow. Define $\dot{v} = DF(x)v$ with initial conditions $v(0) = v_0$. If $v_0 = F(x_0)$ and $v(t) = F(\varphi(t; x_0))$. We want to see if it satisfies:

$$\dot{v}(t) = DF(\varphi(t; x_0)) \cdot v(t) \quad (2.21)$$

$$v(0) = F(x_0) \quad (2.22)$$

Condition 2.22 is directly proved from the definitions and condition 2.21 is also easy to prove using the chain rule:

$$\dot{v}(t) = DF(\varphi(t; x_0)) \frac{d\varphi}{dt}(t; x_0) = DF(\varphi(t; x_0)) \cdot F(\varphi(t; x_0)) = DF(\varphi(t; x_0)) \cdot v(t)$$

Then the Lyapunov exponent in v direction is:

$$\lim_{t \rightarrow \infty} \frac{1}{t} \ln |v(t)| = \lim_{t \rightarrow \infty} \frac{1}{t} \ln |F(\varphi(t; x_0))|$$

Proposition 2.3.0.1. *If the orbit with initial conditions $x(0) = x_0$ is bounded, then there is one zero Lyapunov exponent.*

In the previous point (*Global stability*) we have proved the existence of a trapping region. Therefore we can assume one of the Lyapunov exponents of the Lorenz System to be $h_2 = 0$. In order to find the other two it is only necessary to compute the largest one using the program described in section 4.4 and use the following relation. In dynamical systems where the volume reducing factor is constant, we can derive a relation between the Lyapunov exponents. Since $e^{\sum_i h_i}$ is equal to the volume reduction, this must be equal to the exponential of the divergence of our dynamical system, $e^{\text{div}F}$. So,

$$-\sigma - 1 - b = h_1 + h_2 + h_3 \quad (2.23)$$

For $\sigma = 10$, $b = 8/3$ and $r = 28$ the result is $h_1 \approx 0.9$, $h_2 = 0$, $h_3 \approx -14.57$. Therefore, $h_1 > 0$ and its Lyapunov number is $L_1 = 2.47$ so the distance between a pair of points that start out close together increases by a L_1 factor per unit of time.

Is the attractor periodic? That was also a question that Lorenz asked to himself. In the paper he wrote in 1963, [Lor63] he decided to study the behavior of successive maxima of the z -coordinate. More specifically, he plotted the next maximum of the z -coordinate (z_{n+1}) as a function of the current (z_n). We have repeated this plot with our dates extracted using the Taylor method and the result is shown in figure 3.

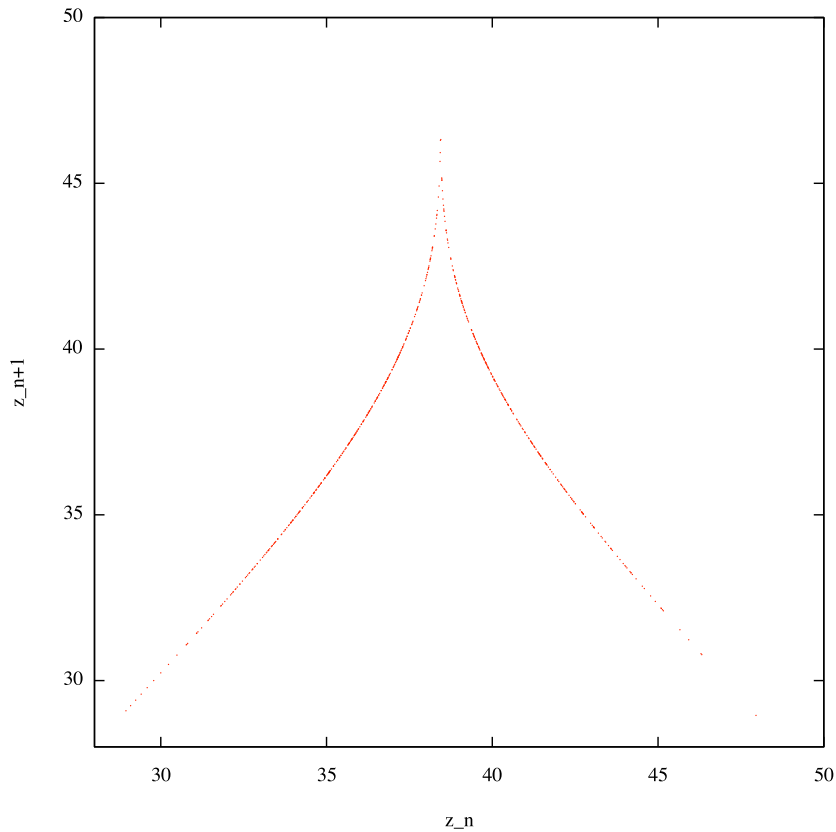


Figure 3: Z-map: Next maximum z_{n+1} as a function of the current maximum z_n

As suggested in [All96] we can say from the plot that the slope of the function is always greater than one so the trajectories will either be non periodic orbits or unstable periodic orbits, but never asymptotically periodic. However, we will go a little bit further. We will do two approximations to study easily the behavior of figure 3. The simplest one will be a tent map and then we will do a real function approximation.

Tent map approximation: The shape of the z-map is similar to a tent map.

$$z_{n+1}(z_n) = \begin{cases} 2z_n & \text{if } z_n \leq \frac{1}{2} \\ 2 - 2z_n & \text{if } z_n \geq \frac{1}{2} \end{cases}$$

The map is continuous but not differentiable at $x = \frac{1}{2}$. To calculate the Lyapunov exponents we will avoid the orbits that map to this point.

$$h = \lim_{n \rightarrow \infty} \frac{1}{n} [\ln |f'(x_1)| + \cdots + \ln |f'(x_n)|] = \lim_{n \rightarrow \infty} \frac{1}{n} \sum_{i=1}^n \ln 2 = \ln 2 \quad (2.24)$$

If the Lyapunov exponent is always positive, $\ln 2$, so proving that the tent map contains chaotic orbits reduces to check that the orbits are not asymptotic periodic orbits. We will use the itineraries method.

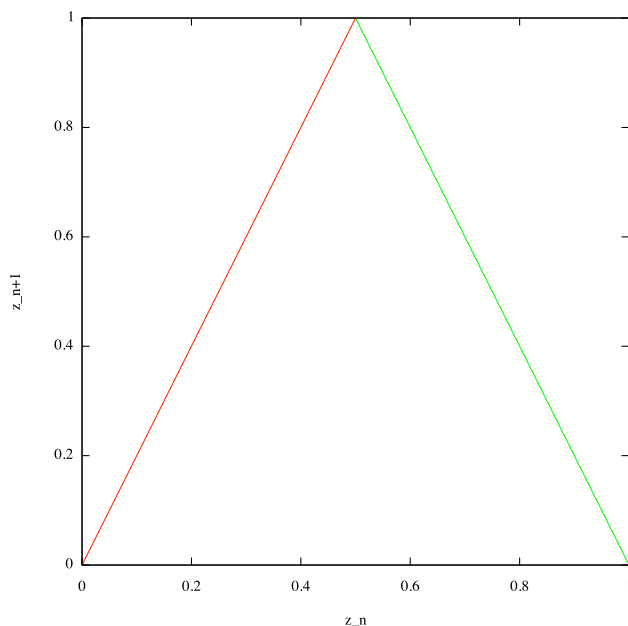


Figure 4: Tent map

We set the left subinterval $L = [0, 1/2]$ and the right subinterval $R = [1/2, 1]$. In the next figure we show a scheme of the itineraries for the tent map. Given an initial point x_0 we construct its itinerary by listing the L or R intervals that contain the point and its further iterations.

As seen in the figure the length of the subintervals is the same in each step. More precisely, a set of points with the same itinerary x_0, \dots, x_k has length 2^{-k+1} . And each of the orbits (which not contain $x = \frac{1}{2}$) corresponds to an itinerary i.e. an infinite sequence of L and R symbols.

So we can show the existence of chaos by proving this theorem, [All96].

Theorem 2.3.0.1. *The tent map T , has infinitely many chaotic orbits*

Proof. The Lyapunov exponent of an orbit of the tent map, as seen before, is $\ln 2$. If an orbit, that avoids $x = \frac{1}{2}$ is not asymptotically periodic, then is a chaotic orbit.

In the tent map, the derivative of T^k at a period- k orbit has module 2^k . For example, the derivative of T^2 at its period-two point $x_0 = 0.3$ is $T'(0.3)T'(0.6) = -4$. This means that all periodic orbits are sources i.e. all orbits sufficiently close to one concrete orbit are repelled from it.

Any asymptotically periodic orbit of the tent map must be eventually periodic and any eventually periodic orbit must have an eventually periodic itinerary. So there exist infinite non repeating itineraries that correspond to distinct chaotic orbits.

□

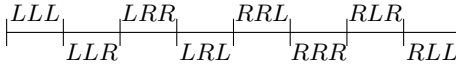
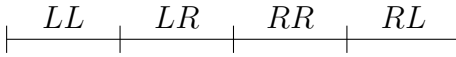
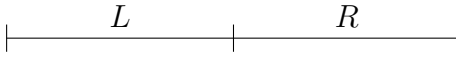
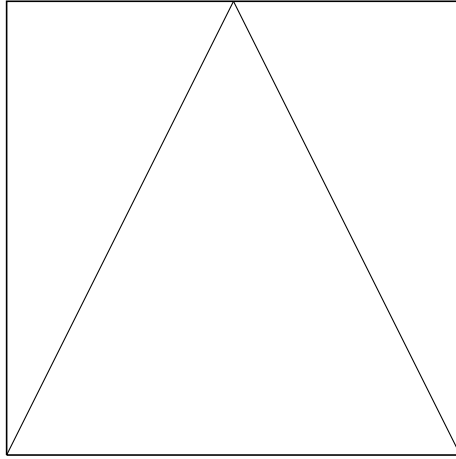


Figure 5: Schematic itineraries for the tent map.

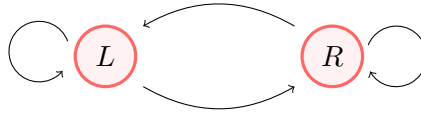


Figure 6: Transition graph map of the tent map T .

Real function approximation: Using *gnuplot* we have reached this approximated function which we will evaluate with the same method that the tent map.

$$z_{n+1}(x) = \begin{cases} -5.00319(38.43515 - z_n)^{0.51372} + 45.5156 & \text{if } 28 < z_n < 38.43515 \\ -4.93892(z_n - 38.43515)^{0.51596} + 45.444 & \text{if } 38.43515 < z_n < 50 \end{cases}$$

If the orbits that contain $z_n \approx 38.43515$ are ignored, then we can compute the Lyapunov exponent, which is approximately 0.679. As in the tent map it is positive. So following an analogous reasoning we arrive at the existence of infinitely many chaotic orbits.

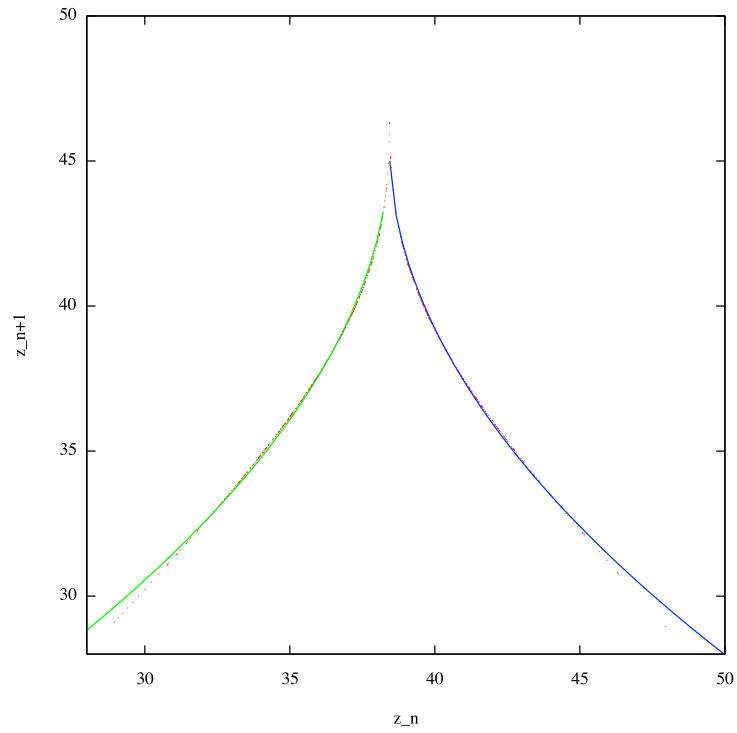


Figure 7: Z -map with approximate functions

Due to the topological similarities between the two approximations and the Z -map we can attribute the characteristics proved to the Z -map, but this does not mean the existence of chaos in the Lorenz attractor. The proof of the existence of chaos is so complicated, [Tuc02], so we will consider that we have signs of it but not the real proof. Even though, and after Tucker's work, we can say that the Lorenz System is locally unstable.

3 Numerical Integration

3.1 Intregation: Taylor method

There exist a bunch of numerical methods to integrate differential equations, for example, the Runge-Kutta methods. In our case, we will use the Taylor method. It is not the most used but it is, as we will see, a great method to obtain accurate results, with a small error and a optimized computational cost. Let us take a look to this method in differential equations solving problems. Consider a Cauchy problem

$$\begin{cases} x'(t) = f(t, x(t)) \\ x(t_0) = x_0 \end{cases}$$

We want to find a smooth function $x : [a, b] \rightarrow \mathbb{R}^m; m \in \mathbb{N}, m > 0$ which is a solution for our problem.

The Theorem of existence and uniqueness of solutions for Cauchy's problem, seen in the course of EDOs, tells us that the function we are searching exists and it's unique. Now we need a method to compute this solution.

Idea of Taylor method: assuming we have an initial condition $x(t_n) = x_n$ we will approximate the value of $x(t_n + h)$ by a Taylor series:

$$\begin{aligned} x(t_0) &= x_0 \\ \vdots \\ x(t_n) &= x_n \\ x(t_n + h) &= x^{(0)}(t_n) + \frac{x^{(1)}(t_n)}{1!}(t_n + h - t_n) + \frac{x^{(2)}(t_n)}{2!}(t_n + h - t_n)^2 + \dots \\ &\quad \dots + \frac{x^{(p)}(t_n)}{p!}(t_n + h - t_n)^p = \\ &= x^{(0)}(t_n) + \frac{x^{(1)}(t_n)}{1!}h + \frac{x^{(2)}(t_n)}{2!}h^2 + \dots + \frac{x^{(p)}(t_n)}{p!}h^p = \sum_{k=0}^{\infty} x^{[k]}(t_n) \cdot h^k \end{aligned} \tag{3.1}$$

In our case, Lorenz equations, the vector x will be a 3-dimensional vector with the cartesian coordinates $x = (x, y, z)$. For this method the only things that we need to compute are the $x^{[i]}(t)$, the normalized derivatives. As we know $x^{[1]}(t)$ we could proceed deriving one and another time this derivatives and using the previous to obtain their expressions. As you can imagine this becomes a difficult, and specially long and complicated, method because at each step the expressions of this derivatives become more and more complex.

So we need to find a different method: *automatic differentiation*.

3.2 Automatic differentiation

Automatic differentiation is a recursive method to calculate the value of the derivatives of certain functions at a given point. These functions have to be obtained by sum, product, quotient or composition of elementary functions (polynomials, trigonometric functions, real powers, exponentials and logarithms). For the Lorenz equations the method is straightforward but we will introduce it to give an idea of how it works. We only need to consider two elementary functions: sum and product of polynomials.

Proposition 3.2.0.2. [Jor01] *If the functions g, h are of class C^m then we have:*

$$\begin{aligned} \text{If } f(t) = g(t) \pm h(t), \text{ then } f^{[n]}(t) &= g^{[n]}(t) \pm h^{[n]}(t) \\ \text{If } f(t) = g(t) \cdot h(t), \text{ then } f^{[n]}(t) &= \sum_{i=0}^n g^{[n-i]}(t) \cdot h^{[i]}(t) \end{aligned}$$

where $f^{[i]}(t) = \frac{f^{(i)}(t)}{i!}$ is the *normalized i -th derivative*. (idem for $g^{[i]}(t)$ and $h^{[i]}(t)$)

3.3 Step size control and degree

As we have explained, we are using the Taylor method to integrate the equations and following the paper [Jor01]. So, given an initial value of the time t_n and its coordinates $x(t_n)$ we want to compute the coordinates for the next point in the trajectory $x(t_n + h)$. We will approximate it by a Taylor series but, which has to be the p -order of the series? And, what is more, how big has to be the *step size* $= h$ to obtain an error of the approximation less than a certain tolerance, ε , but at the same time have an efficient program. In other words, we have to choose a value of h and p , such that:

$$\|x(t_n + h) - x^{[\leq p]}(t_n + h_n)\| \leq \varepsilon, \forall n$$

where $x^{[\leq p]}(t_n + h_n)$ is the truncated Taylor series at order p . More precisely, we are going to choose a h_n for each n , so each step will have the optimized size. So h_n and p will be those such that:

1. $\|x(t_n + h_n) - x^{[\leq p]}(t_n + h_n)\| \leq \varepsilon, \forall n$
2. The total number of operations of the numerical integration is as small as possible.

If we break our Taylor series in the p order we can approximate the error by the first (of the maximum between the two first) terms after the truncation:

$$\begin{aligned} x(t_n + h_n) &= \sum_{k=0}^p x_k \cdot h^k + \sum_{k>p}^{\infty} x_k \cdot h^k \\ \text{error} &\approx \max(|x_{p+1}| h^{p+1}, |x_{p+2}| h^{p+2}) \leq \varepsilon \end{aligned}$$

$$h \leq \sqrt[p+1]{\frac{\varepsilon}{|x_{p+1}|}} \text{ or } h \leq \sqrt[p+2]{\frac{\varepsilon}{|x_{p+2}|}}$$

From now on, and to simplify notation, we consider that the error is $|x_{p+1}|h^{p+1}$. The result for error $\approx \max(|x_{p+1}|h^{p+1}, |x_{p+2}|h^{p+2}) = |x_{p+2}|h^{p+2}$ would be the same replacing $p+1$ with $p+2$.

$$h \approx \sqrt[p+1]{\frac{\varepsilon}{|x_{p+1}|}} \approx \varepsilon^{\frac{1}{p+1}} \cdot \rho$$

where ρ is an approximation of the radius of convergence of the series. On the other hand, we have to consider the computational effort.

Corollari 3.3.0.1. *The number of arithmetic operations to compute the derivatives up to order p of a vector field written by elementary functions is of $O(p^2)$.*

Using the previous corollary for the Lorenz system, the number of arithmetic operations we need to obtain the derivatives up to order p is of $O(p^2) \approx A \cdot (p+1)^2$. So the number of operations per unit of time is:

$$o(p) = \frac{A \cdot (p+1)^2}{h} = \frac{A \cdot (p+1)^2}{\varepsilon^{\frac{1}{p+1}} \cdot \rho}$$

If we differentiate this expression as a function of p and we equal it to zero to minimize it we obtain:

$$o'(p) = \frac{A}{\rho} \left(\frac{2 \cdot (p+1) \cdot \varepsilon^{\frac{1}{p+1}} - (p+1)^2 \cdot \ln(\varepsilon) \cdot \varepsilon^{\frac{1}{p+1}} \left(-\frac{1}{(p+1)^2} \right)}{\varepsilon^{\frac{2}{p+1}}} \right)$$

$$\text{If } o'(p) = 0 \rightarrow 2 \cdot (p+1) + \ln(\varepsilon) = 0 \rightarrow p = -\frac{1}{2} \ln(\varepsilon) - 1$$

$$\text{when } \varepsilon \rightarrow 0 \implies \boxed{p \approx -\frac{1}{2} \ln(\varepsilon)}$$

Finally,

$$h \approx \varepsilon^{\frac{1}{p+1}} \cdot \rho \approx \varepsilon^{\frac{-2}{\ln(\varepsilon)}} \cdot \rho = \frac{\rho}{e^2}$$

Observation 1. The value of h can be very big, is what we call a dangerous step size because it can create big errors or a wrong approximation, see more in [Jor01]. To avoid this situation we are going to use a parameter control in our program. So if when calculating the step size it is bigger than a given value h^* (in our case $h^* = 0.01$) then we will use automatically h^* as the step size.

3.4 Example: The Lorenz System

In our specific case, as we said, the difficulty is really low. Nevertheless as the automatic differentiation is a really useful method we will use it for the computation of Lorenz equations. To use the Taylor method we need to compute the n -derivates of the coordinates $(x(t), y(t), z(t))$ from the equations. After we will discuss the degree of truncation of the Taylor series to optimize the computation and fit the solution with a fixed error. Using the automatic differentiation we obtain the following formulas for the computation of the derivatives:

$$\begin{aligned}
 x^{[n]}(t) &= \frac{\sigma}{n+1} (y^{[n-1]}(t) - x^{[n-1]}(t)) \\
 y^{[n]}(t) &= \frac{1}{n+1} \left(-y^{[n-1]}(t) + \rho \cdot x^{[n-1]}(t) - \sum_{i=0}^n x^{[n-i]}(t) \cdot z^{[i]}(t) \right) \\
 z^{[n]}(t) &= \frac{1}{n+1} \left(-b \cdot z^{[n-1]}(t) + \sum_{i=0}^n x^{[n-i]}(t) \cdot y^{[i]}(t) \right)
 \end{aligned}$$

As we know $(x^{[1]}(t), y^{[1]}(t), z^{[1]}(t))$ we can compute all the other derivatives to construct the Taylor series of each coordinate.

We have developed two different programs using C code. The first one to compute the integration explained, taking into account the calculation of the most suitable *step size* in each time step. We also have introduced a Newton's method to calculate accurately the maximums of the z coordinate used in section 2.3 to plot the one dimensional Z -map. Once we had the integration method we developed the second program to calculate the largest Lyapunov exponent of the Lorenz equations following the method explained in [Bov04].

We have done different computations of the Lorenz attractor. In the following figures appears a sample of them. The error chosen is $\varepsilon = 10^{-21}$ and then $p = 25$ in concordance with the expressions deduced in the previous section. Some other choices we had made are: the value of the parameters is the same as Lorenz used in his work: $r = 28$, $\sigma = 10$ and $b = \frac{8}{3}$, we have used different initial conditions, here are shown results for $(x_0, y_0, z_0) = (0.6, 0.6, 0.7)$ and $(x_0, y_0, z_0) = (-1.2, 0.9, 0.1)$, the integration time generally is $t = 1000$ but we have done some computations with $t = 10000$ and the control parameter $h^* = 0.01$ has been changed for $h^* = 0.001$ in one of the cases.

See the results in next page.

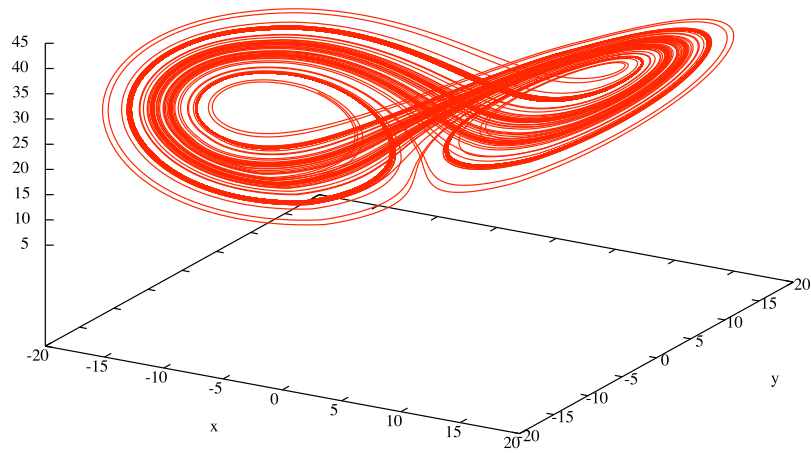


Figure 8: Lorenz attractor with $h^* = 0.01$ and computation time $t = 10000$.

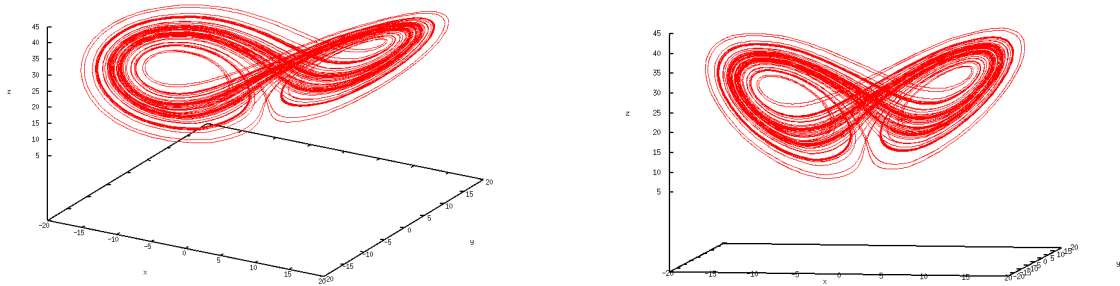


Figure 9: Lorenz attractor with $h^* = 0.01$ and computation time $t = 1000$.

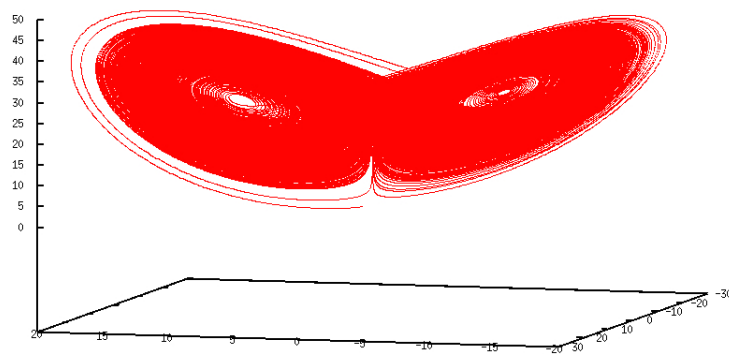


Figure 10: Orbit ending in the Lorenz attractor with i.c. $(0.6, 0.6, 0.7)$, $h^* = 0.001$ and computation time $t = 10000$.

Observations: we have dropped out the first terms of the integration since they do not belong to the Lorenz attractor. It is also visible that an increase in the integration time can have two effects. In figure 8 the Lorenz attractor is better defined since it has done some more orbits than in 9. On the other hand, in figure 10 the attractor is difficult to see, this occurs because the step size control parameter is smaller ($h^* = 0.001$) and the orbits are more accurate from the beginning, hence it is not necessary a long integration time.

4 The parameterization method for invariant manifolds

First of all we will give a general theoretical framework of the method of parameterization for flows, [Cab04]. Then we will focus on the computation of the parameterized invariant manifolds of a vector field, [Har10].

4.1 The parameterization method for flows

Consider an n -dimensional vector field, $F : U \rightarrow \mathbb{R}^n$

$$\dot{x} = F(x) \tag{4.1}$$

where the vector field $F(x)$ is in $U \subset \mathbb{R}^n$, U is an open set containing the origin and $F(0) = 0$.

If V^L is a subspace of \mathbb{R}^n of dimension d invariant by $DF(0)$. In this method we look for a parameterization.

$$W : U_1 \subset V^L \longrightarrow \mathbb{R}^n \tag{4.2}$$

and a vector field f , $f : U_1 \rightarrow \mathbb{R}^d$, in $U_1 \subset V^L$ such that

$$F \circ w = DK \cdot f \tag{4.3}$$

At the range of K , the vector field F is tangent to the range of K . This means that the range of K is invariant under the flow of F . What is more, the vector field f is the representation in parameters of the restriction of X to the invariant manifold.

4.2 Manifolds associated to a fixed point of a vector field

It is necessary to introduce some terminology used in the following section.

We say that a function is in C^ω if it is analytic.

The spectrum of a linear operator Λ in \mathbb{R}^n is denoted by $\text{Spec}(\Lambda)$ which is a compact subset of \mathbb{C} .

For $j \in \mathbb{N}$ and $S \subset \mathbb{C}$ we use the notation:

$$jS := \{a_1 + \cdots + a_j | a_i \in S\}$$

Consider a vector field $F(z)$ in $U \subset \mathbb{R}^n$ such that $F(0) = 0$, and a linear subspace $V^L \subset \mathbb{R}^n$ invariant under $DF(0)$. Now consider the correspondent invariant manifold under the flow of F which passes through the origin and it is tangent to V^L in this point.

Theorem 4.2.0.2. *Let F be a C^ω vector field on an open set U of \mathbb{R}^n with $0 \in U$, such that $F(0) = 0$. Let $\Lambda = DF(0)$ and $M \in \mathbb{N}$, $M \geq 1$. Suppose that:*

1. *There is a linear subspace V^L of \mathbb{R}^n such that $\Lambda(V^L) \subset V^L$. Hence there is a decomposition $\mathbb{R}^n = V^L \oplus V^N$ and, with respect to it, Λ has de form*

$$\begin{pmatrix} \Lambda_L & T \\ 0 & \Lambda_N \end{pmatrix} \tag{4.4}$$

where, in our case, $\Lambda_L = \text{diag}(\lambda_1, \dots, \lambda_d)$.

2. *$\text{Spec}(\Lambda_L) \subset \{z \in \mathbb{C} | \text{Re}(z) < 0\}$.*
3. *$j\text{Spec}(\Lambda_L) \cap \text{Spec}(\Lambda_N) = \emptyset$ for $j \geq 2$.*

Then, there exist a C^ω map $K : U_1 \subset E \rightarrow \mathbb{R}^n$, where U_1 is a neighborhood of 0 in V^L , and a linear $f : V^L \rightarrow V^L$, $f(s) = \Lambda_L s$, such that

$$F \circ W = DW \cdot f \text{ in } U_1, \tag{4.5}$$

$$W(0) = 0, DW(0)V^L = V^L, \tag{4.6}$$

$$f(0) = 0, Df(0) = \Lambda_L \tag{4.7}$$

4.3 Computation of Invariant Manifolds

The computation of invariant manifolds will be done using the parametrization method explained in the following section. We will introduce the invariance equation and from it some different ways of parametrizing. Finally we will apply this method for the specific case of the Lorenz System, [Har10].

4.3.1 The invariance Equation

In this section we want to compute a high order approximation, later we will discuss which has to be this order, of an invariant manifold for a n -dimensional vector field. We have tried to be consistent with the notation used in 4.1

Consider an n -dimensional vector field

$$\dot{z} = F(z) \tag{4.8}$$

where its coordinates are $z = (z_1, \dots, z_n)$ and let $z^* \in \mathbb{C}^n$ be a fixer point of it. Then, let $V^L \subset \mathbb{C}^n$ be a d -dimensional subspace invariant for the linearization $DF(z^*)$ around the fixed point z^* . Let W be a parameterization of d -dimensional invariant manifold for $\dot{z} = F(z)$ tangent to the subspace V^L in z^* .

The parameterization method consists in finding an expression of the way $z = W(s)$ of the d -dimensional invariant manifold \mathfrak{W} , where $s = (s_1, \dots, s_d)$ are the coordinates of the manifold. We can also point that $W(0) = z^*$, since it is tangent to V^L in z^* , as said before. The dynamics on the manifold will be described as a function of he coordinates s , $\dot{s} = f(s)$ with $f(0) = 0$.

The invariance equation is,

$$F(W(s)) = DW(s)f(s) \tag{4.9}$$

We can prove easily the validity of this expression by using the elements described: $F(W(s)) = \dot{W}(s) = DW(s)\dot{s} = DW(s)f(s)$.

The approximation of the manifold will be of the form:

$$W(s) = W(0) + \sum_{k \geq 1} W_k(s) = z^* + \sum_{k \geq 1} W_k(s) \tag{4.10}$$

where W_k is a n -dimensional vector of homogeneous polynomials of degree k and d -variables.

We also want to approximate the dynamics in the manifold, so we will do it the same way.

$$f(s) = f(0) + \sum_{k \geq 1} f_k(s) = \sum_{k \geq 1} f_k(s) \tag{4.11}$$

where f_k is a d -dimensional vector of homogeneous polynomials of degree k and d -variables.

To compute this high approximations we will use the Invariance Equation but we have to introduce some changes.

Consider $L \in \mathbb{C}^{n \times d}$, the matrix whose column vectors are the vectors of the the subspace V^L . Now, consider an invertible P matrix obtained by joining L and

a matrix $N \in \mathbb{C}^{n \times (n-d)}$. The column vectors of N span a $(n-d)$ -dimensional subspace $V^N \subset \mathbb{C}^n$ and complementary to V^L . This subspace can be also invariant under the linearized flow or not, we will see later the condition.

With the help of this new matrix, P , we can define the matrix Λ as follows,

$$\Lambda = P^{-1}DF(z^*)P = \begin{pmatrix} \Lambda_L & T \\ 0 & \Lambda_N \end{pmatrix} \quad (4.12)$$

where $\Lambda_L \in \mathbb{C}^{d \times d}$, $\Lambda_N \in \mathbb{C}^{(n-d) \times (n-d)}$ and $T \in \mathbb{C}^{d \times (n-d)}$ is the torsion matrix. If V^N is invariant under the linearized flow then the torsion is zero. The eigenvalues of Λ_L will be called *tangent eigenvalues* and the eigenvalues of Λ_N , *normal eigenvalues*. In this section we will make the assumption that Λ_L and Λ_N are diagonal, so we can express them as: $\Lambda_L = \text{diag}(\lambda_1, \dots, \lambda_d)$ and $\Lambda_N = \text{diag}(\lambda_{d+1}, \dots, \lambda_n)$.

The linear terms (the first order ones) of the approximation of $W(s)$ and $f(s)$ are already known:

$$W_1(s) = Ls \quad (4.13)$$

$$f_1(s) = \Lambda_L s \quad (4.14)$$

in the next section we will find a procedure to find the higher order terms.

4.3.2 The Cohomological Equations

First of all we have to find a way of solving the equation 4.9. We will proceed with a recursive method. In each step we are going to find the homogeneous polynomials of degree k by using the previous polynomials of degree $\leq k$. So, we suppose to have computed the $k-1$ order terms of the equation 4.9 and we will write them as $[F(W(s)_{<k})]_{<k}$. Our goal is to compute the term $[F(W(s)_{<k})]_k$.

Substituting the approximations for $W(s)$ and $f(s)$, equations 4.10 and 4.11, in the Invariance Equation we obtain:

$$F(W_{<k}(s) + W_k(s) + \dots) = D(W_{<k}(s) + W_k(s) + \dots)(f_{<k}(s) + f_k(s) + \dots) \quad (4.15)$$

As we only want to compute de term of order k we will only take the terms of the expression with this order. In the left hand side of 4.15 we do Taylor around $W_{<k}(s)$.

$$F(W_{<k}(s) + W_k(s) + \dots) = F(W_{<k}(s)) + DF(W_{<k}(s))(W_k(s) + \dots) + \dots$$

The only terms of k order in the left handside are:

$$[F(W_{<k}(s))]_k + DF(z^*)W_k(s)$$

In the right side of 4.15 we will only take the terms of order k :

$$[DW_{<k}(s)f_{<k}(s)]_k + DW_k(s)f_1(s) + DW_1(s)f_k(s)$$

Finally, the Cohomological Equation for W_k and f_k is:

$$[F(W_{<k}(s))]_k + DF(z^*)W_k(s) = [DW_{<k}(s)f_{<k}(s)]_k + DW_k(s)f_1(s) + DW_1(s)f_k(s) \quad (4.16)$$

Reorganizing and substituting 4.13 and 4.14,

$$DF(z^*)W_k(s) - DW_k(s)\Lambda_L s - Lf_k(s) = [DW_{<k}(s)f_{<k}(s)]_k - [F(W_{<k}(s))]_k = -E_k(s) \quad (4.17)$$

where we have defined a order- k error term, $E_k(s) = [F(W_{<k}(s))]_k - [DW_{<k}(s)f_{<k}(s)]_k$. Defining the n -dimensional vectors $\xi_k(s) = P^{-1}W_k(s)$ and $\eta_k(s) = -P^{-1}E_k(s)$ the equation 4.17 becomes:

$$\begin{aligned} P^{-1}DF(z^*)P\xi_k(s) - P^{-1}PD\xi_k(s)\Lambda_L s - P^{-1}Lf_k(s) &= -P^{-1}E_k(s) \\ \rightarrow \Lambda\xi_k(s) - D\xi_k(s)\Lambda_L s - \begin{pmatrix} I_d \\ 0 \end{pmatrix} f_k(s) &= \eta_k(s) \end{aligned} \quad (4.18)$$

The notation used for the n -dimensional vectors of order k is the following, where each component is an homogeneous polynomial of degree k .

$$\begin{aligned} \xi_k(s) &= (\xi_k^1(s), \dots, \xi_k^n(s)) \\ \eta_k(s) &= (\eta_k^1(s), \dots, \eta_k^n(s)) \\ f_k(s) &= (f_k^1(s), \dots, f_k^d(s)) \end{aligned}$$

From 4.18 the normal and the tangent cohomological equations are obtained. Writing metrically the equation 4.18 it is easier to see.

$$\begin{pmatrix} \Lambda_L & T \\ 0 & \Lambda_N \end{pmatrix} \begin{pmatrix} \xi_k^L(s) \\ \xi_k^N(s) \end{pmatrix} - \begin{pmatrix} D\xi_k^L(s)\Lambda_L s \\ D\xi_k^N(s)\Lambda_L s \end{pmatrix} - \begin{pmatrix} f_k(s) \\ 0 \end{pmatrix} = \begin{pmatrix} \eta_k^L(s) \\ \eta_k^N(s) \end{pmatrix} \quad (4.19)$$

$$\text{Normal cohomological equation : } \Lambda_N \xi_k^N(s) - D\xi_k^N(s)\Lambda_L s = \eta_k^N(s) \quad (4.20)$$

$$\text{Tangent cohomological equation : } \Lambda_L \xi_k^L(s) - D\xi_k^L(s)\Lambda_L s - f_k(s) = \eta_k^L(s) - T\xi_k^N(s) \quad (4.21)$$

Solving each equation we will compute the k -order homogeneous polynomials $\xi_k^N(s)$, $\xi_k^L(s)$, $f_k(s)$. And from these the $k + 1$ component of $\eta_{k+1}(s)$ that will lead us to the next step.

Normal cohomological equation. Equation 4.20 is written:

$$\lambda_i \xi_k^i(s) - D\xi_k^i(s)\Lambda_L s = \eta_k^i(s) \quad (4.22)$$

for $i = d + 1, \dots, n$ and using the diagonal expression for Λ_N . These equations are diagonal in the coefficients ξ_m^i of the homogeneous polynomials $\xi_k^i(s)$, where¹ $m = (m_1, \dots, m_d)$, $|m| = m_1 + \dots + m_d = k$. So, for $i = d + 1, \dots, n$ and $|m| = k$:

$$(\lambda_i - \lambda_L m)\xi_m^i = \eta_m^i \Rightarrow \xi_m^i = \frac{\eta_m^i}{\lambda_i - \lambda_L m} \quad (4.23)$$

where $\lambda_L m = \lambda_1 m_1 + \dots + \lambda_d m_d$. The equation can be solved unless there are *cross resonances*, i.e. pairs $(m, i) \in \mathbb{N} \times \{d + 1, \dots, n\}$ with $|m| \geq 2$ such that $\lambda_i = \lambda_L m$.

Tangent cohomological equation. Equation 4.21 is written:

$$\lambda_i \xi_k^i(s) - D\xi_k^i(s)\Lambda_L s - f_k(s) = \eta_k^i(s) - T\xi_k^i(s) \quad (4.24)$$

for $i = 1, \dots, d$ and using the diagonal expression for Λ_N . With the same procedure as for the normal equations we obtain:

$$(\lambda_i - \lambda_L m)\xi_m^i - f_m^i = \eta_m^i - T\xi_m^i \Rightarrow \xi_m^i = \frac{\eta_m^i - T\xi_m^i + f_m^i}{\lambda_i - \lambda_L m} \quad (4.25)$$

The equation can be solved unless there are *internal resonances* i.e. pairs $(m, i) \in \mathbb{N} \times \{1, \dots, d\}$ with $|m| \geq 2$ such that $\lambda_i = \lambda_L m$

4.3.3 The Normal Form Style

There are different styles of parameterization. One of them is *The Graph Style*. It consists in parameterizing the manifold in the simplest possible way by taking $\xi_k^L(s) = 0$ and $f_k(s) = -\eta_k^i(s) + T\xi_k^i(s)$.

Another one is *The Normal Form Style*. In this case the simplified expression is in the dynamics on the manifold. To simplify the expression of $f_k(s)$ we will find a normal form for it, in the case of non-resonances the internal vector field is linear. This means that for $i = 1, \dots, d$, $|m| = k$:

¹A multi index notation is introduced

$$\begin{cases} f_m^i = 0 \text{ and } \xi_m^i = \frac{\eta_m^i - T\xi_m^i}{\lambda_i - \lambda_L m} & \text{if } \lambda_i \neq \lambda_L m \\ f_m^i = -\eta_m^i + T\xi_m^i \text{ and } \xi_m^i = 0 & \text{if } \lambda_i = \lambda_L m \end{cases} \quad (4.26)$$

It is useful specially in cases with a finite number of resonances, or in our case, without resonances. Hence dynamics on the manifold can be described by a polynomial vector field. The most suitable situations occur when working with stable or unstable manifolds because the d internal eigenvalues lie all in the half-plane or in the right-plane.

4.4 Example: Lorenz System

Now we will use the method of parameterization using the normal form style to compute the stable manifold of dimension 2 of the Lorenz System described in 2.2. The parameters of the equations used are $\sigma = 10$, $r = 28$ and $b = \frac{8}{3}$.

Summing up the information needed: this dynamical system has simple characteristics that makes it an easy example for the parameterization. It has three fixed points but we will take the origin (henceforth $z^* = (0, 0, 0)$). The three eigenvalues of the differential matrix of the vector field around the origin are:

$$\begin{aligned} \lambda_1 &= \frac{-1 - \sigma - \sqrt{(\sigma + 1)^2 - 4\sigma(1 - r)}}{2} = -22.82772 \\ \lambda_2 &= -b = -2.66667 \\ \lambda_3 &= \frac{-1 - \sigma + \sqrt{(\sigma + 1)^2 - 4\sigma(1 - r)}}{2} = 11.82772 \end{aligned}$$

From the eigenvalues we can affirm that there are no possible resonances. The dimension of the vector field is $n = 3$ and the dimension of the manifold $d = 2$, therefore the coordinates of the parameterization will be $s = (s_1, s_2)$ and $\xi_1(s) = (s_1, s_2, 0)$. The P matrix has as columns the unitary eigenvectors of eigenvalues λ_1 , λ_2 and λ_3 in this order. P^{-1} is its inverse matrix.

We have decided to compute the parameterization using the normal form style described in section 4.3.3, thus the dynamics on the manifold will be described by the simplest possible form of $f(s)$ which will be linear: $f(s) = (\lambda_1 s_1, \lambda_2 s_2)$. Since the torsion is zero and $f(s)$ has only linear part, the tangent equations become so simple and similar to the normal equations. At this point starts the computation of the proceeding components of the vectors $\xi_k(s)$ and $\eta_k(s)$, with $k \geq 2$. We need to remember that $\xi(s)$, $\eta(s)$, $W(s)$ are vectors of three components and that $\xi_k(s)$, $\eta_k(s)$, $W_k(s)$ are the homogeneous polynomials of degree k for each component.

$$\begin{aligned} \xi_k(s) &= (\xi_k^1(s), \xi_k^2(s), \xi_k^3(s)) \\ \eta_k(s) &= (\eta_k^1(s), \eta_k^2(s), \eta_k^3(s)) \\ f_k(s) &= (f_k^1(s), f_k^2(s), f_k^3(s)) \end{aligned}$$

The steps that our program will follow are:

Computation of the homogeneous polynomials of degree $k = 2$ knowing $\xi_1(s)$ already.

1. From $\xi_1(s)$ we obtain $W_{<2}(s) = W_1(s) = z^* + P\xi_{<2}(s) = P\xi_{<2}(s) = P\xi_1(s)$.
2. Then it calculates the order-2 error term: $E_2(s) = [F(W_{<2}(s))]_2 - [DW_{<2}(s)f_{<2}(s)]_2 = [F(P\xi_{<2}(s))]_2 - [DW_{<2}(s)(\lambda_1 s_1, \lambda_2 s_2)]_2$. Notice that the second term is not needed to be calculated. Since $f_{<k}(s) = (\lambda_1 s_1, \lambda_2 s_2), \forall k > 0$, and $f_k = 0, \forall k > 2$, the term will never reach the k -order. Then, in this step the error is calculated with the simpler expression: $E_2(s) = [F(P\xi_{<2}(s))]_2$. We also notice that the only parts of the vector field important in this computation are the multiplying terms (xz and xy in the second and the third equation respectively). The other ones can never reach order k .
3. From $E_2(s)$ we obtain $\eta_k(s) = -P^{-1}E_2(s)$.
4. Because there are no resonances the last calculation is also simple: $\xi_m^i = \frac{\eta_m^i}{\lambda_i - \lambda_L m}$ for $i = 1, 2, 3$ and $|m| = 2$. The normal equation and the tangent equation become the same and $\lambda_L m = \lambda_1 m_1 + \lambda_2 m_2$.

Now we can move forward and compute the homogeneous polynomials of degree $k = 3$ and go one until the last k order. Knowing $W_2(s)$ we can start again the process from step 1 to 4. It is really important in step 2 to take into account all the components and degree of $W_{<k}$ since they can become relevant in the multiplying terms.

4.4.1 Maximum order and error

We have mentioned that the parameterization method computes a high order approximation of the invariant manifold, but which is this order? As we did in Taylor's method, it is necessary to find a balance between the error and the computational cost. Now we will give relevance to the size of the fundamental domain in which the approximation is sufficiently accurate and therefore which is highly related with the order of the expansion. To visualize it is plotted the relation between the error (ε) and the size of the fundamental domain (δ). They are related by:

$$\varepsilon(\delta) = \max_{\theta \in [0, 2\pi)} e_0(t, s_{\delta, \theta}) \quad (4.27)$$

where $s_{\delta, \theta} = (\delta \cos \theta, \delta \sin \theta)$ (another option could have been to use a square domain). We have chosen the same time step $t = 0.3$ as in [Har10], to have a maximum backward-time expansion factor of 1000. e_0 is the *error in the orbit*, defined as:

$$e_0(t, s_0) = |W(s(t)) - z(t)|_\infty \quad (4.28)$$

where s_0 is an initial condition s.t. $z_0 = W(s_0)$ and $z(t)$ and $s(t)$ are the numerical solutions of $\dot{z} = F(z)$, $z(0) = z_0$ and $\dot{s} = f(s)$, $s(0) = s_0$, respectively.

We have compute the error for different values of k , the order of the approximation of $W(s)$.

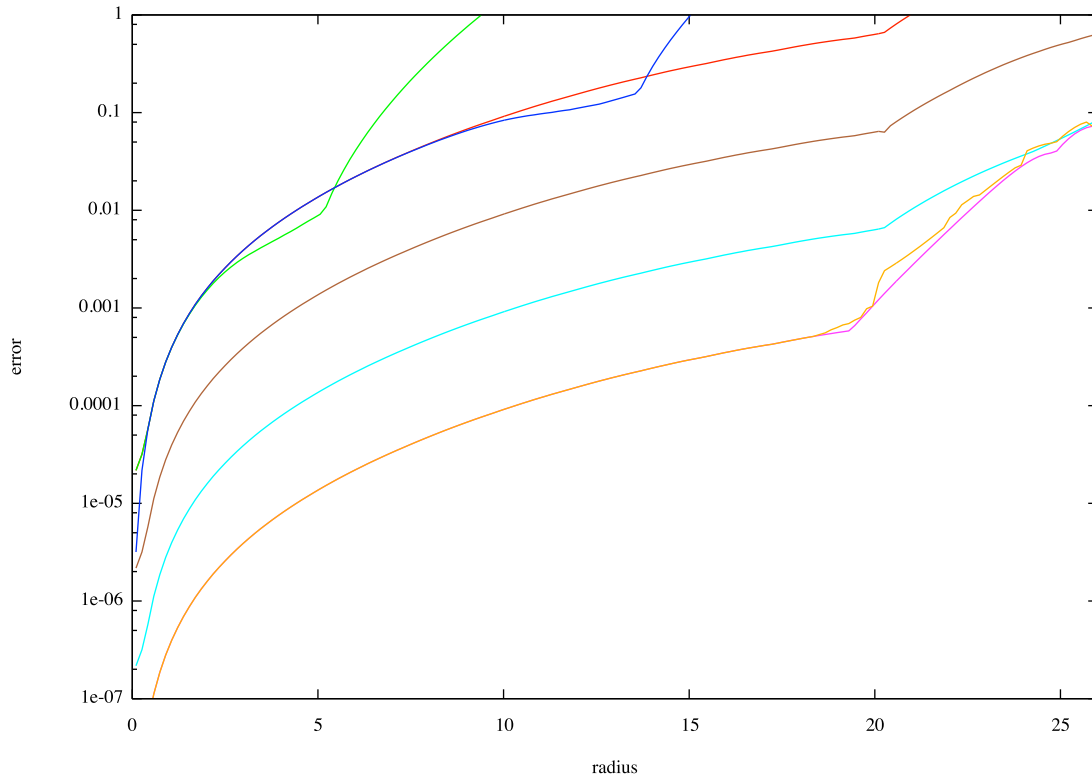


Figure 11: Error ε of the approximation of the invariant manifold $\mathfrak{W}^s(P_0)$ as a function of the radius δ of the fundamental domain, for different orders. Each curve represents a different order k . From lower right to top left: $k = 60, 50, 40, 30, 20, 10, 5$.

4.5 Results

With this results we have chosen an expansion order of $k = 50$ because we have observed that is really similar to the upper orders and a $\delta = 20$. The error obtained then is approximately of order $\varepsilon \approx 10^{-4}$. Now we will plot the expansion of the stable manifold with different shapes of the fundamental domain. It is also important to emphasize that with this representation we also calculate the slow submanifold (given by $s_1 = 0$) inside the stable manifold.

- (a) **Squared domain** We have taken $s_1 \in [-20, 20]$ and $s_2 \in [-20, 20]$ spaced by a factor $d = 0.1$ or $d = 0.5$.

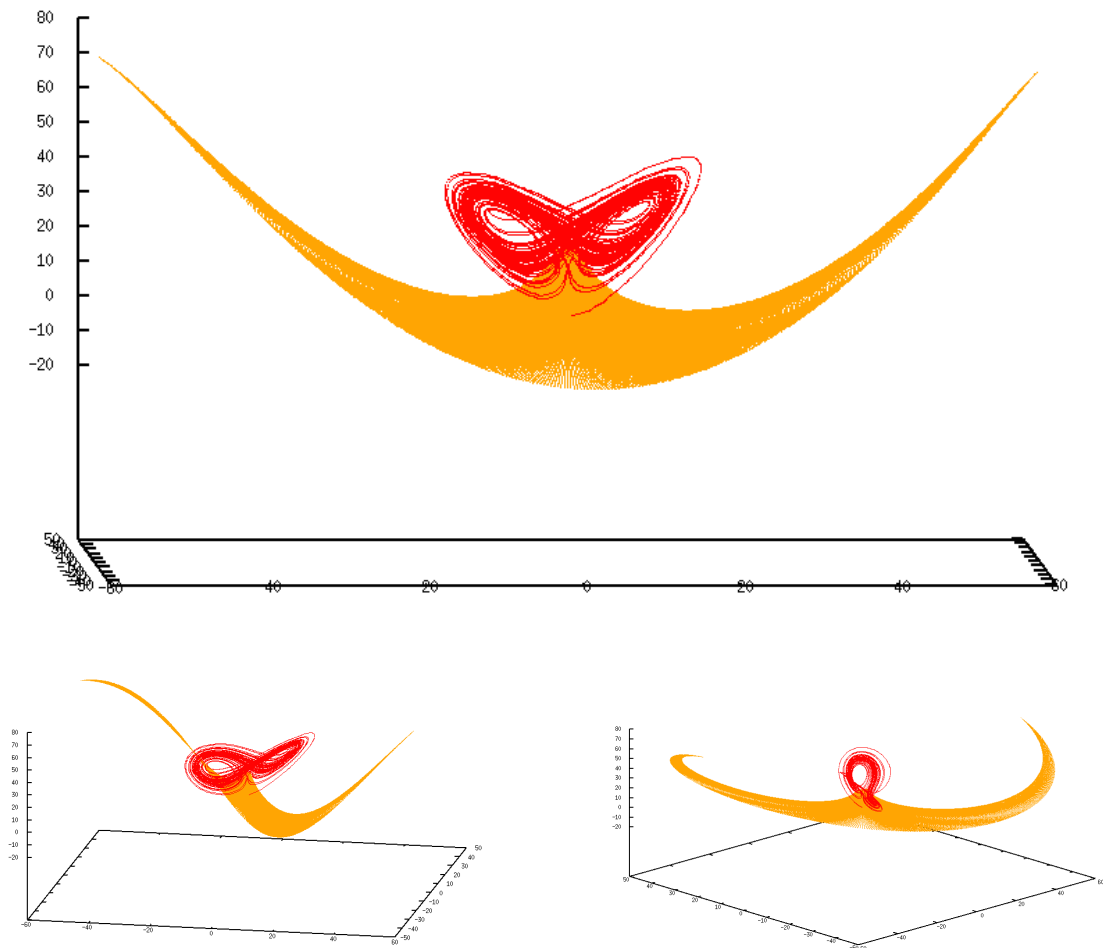


Figure 12: In red: Lorenz attractor. In orange: the expansion of the stable manifold in a squared fundamental domain of length $\delta = 20$ and with $d = 0.1$.

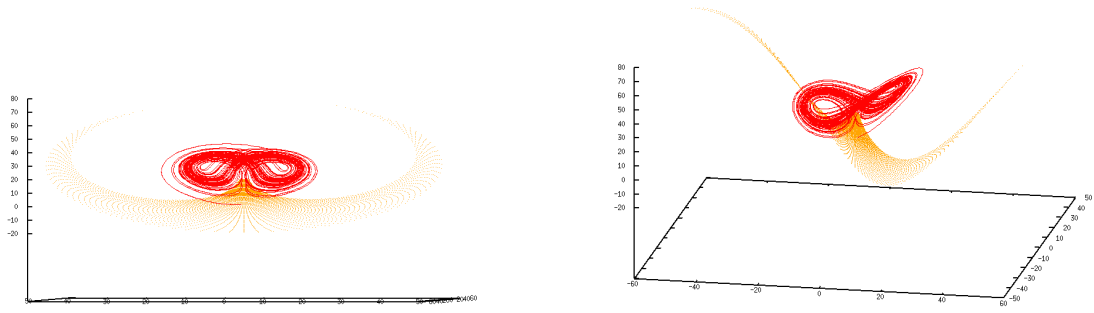


Figure 13: In red: Lorenz attractor. In orange: the expansion of the stable manifold in a squared fundamental domain of length $\delta = 20$ and with $d = 0.5$.

(b) **Circular domain** We have taken 250 values of δ equally spaced in $[0.1, 20]$ and 100 values of θ equally spaced in $[0, 2\pi]$. Then the coordinates of the parameterization are:

$$(s_1, s_2) = (\delta \cos \theta, \delta \sin \theta)$$

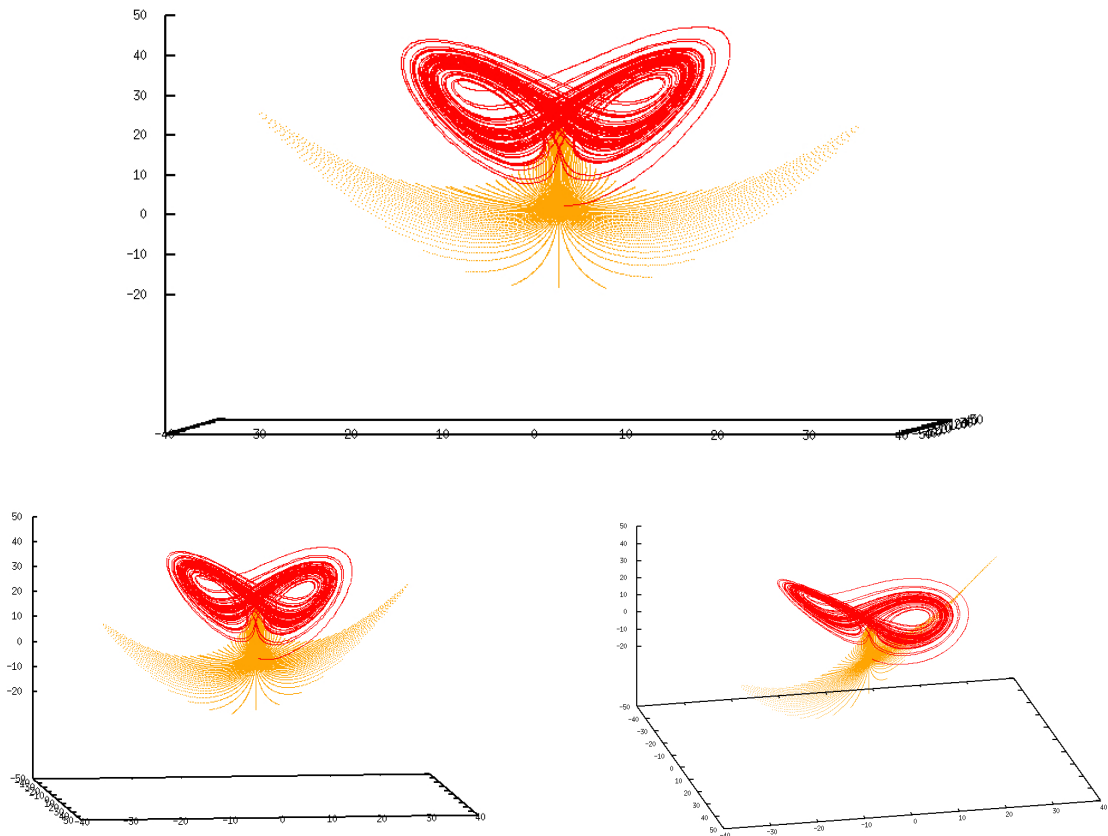


Figure 14: In red: Lorenz attractor. In orange: the expansion of the stable manifold in a circular fundamental domain of radius $\delta = 20$.

(c) **Circular domain with orbits** In this last case we have repeated the previous plot but we have used specific (s_1, s_2) . Instead of covering all the circular domain we have taken the initial conditions in the border of the domain $s(0) = (s_{10}, s_{20}) = (20 \cos \theta, 20 \sin \theta)$ and we have plotted the trajectory of each initial condition according to the dynamics in the manifold.

$$\begin{cases} \dot{s}_1 = \lambda_1 s_1 \rightarrow s_1(t) = s_{10} e^{\lambda_1 t} \\ \dot{s}_2 = \lambda_2 s_2 \rightarrow s_2(t) = s_{20} e^{\lambda_2 t} \end{cases} \quad (4.29)$$

We have plot from $t = 0$ until $t = 1$ with a step size of 0.001.

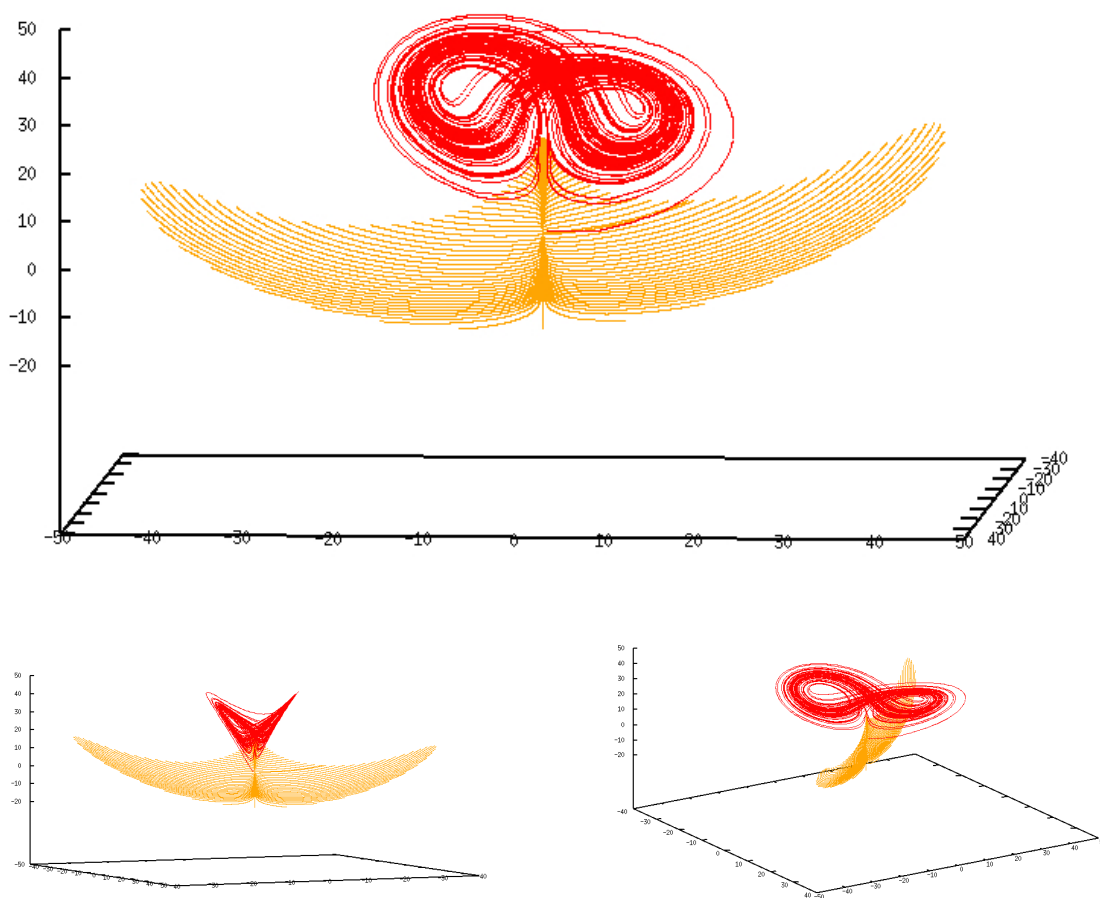


Figure 15: In red: Lorenz attractor. In orange: the expansion of the stable manifold in a circular fundamental domain of radius $\delta = 20$ with several trajectories in the manifold.

5 Conclusions

We began this paper with an introduction based on Lorenz's work in the 1960s, when he discovered through a small experiment an important property of the Lorenz system: its sensitive dependence on initial conditions. From that moment on, the chaotic theory has evolved so much, that we have had to focus this work on certain specific areas. We have only treated the aspects we considered more interesting for the goal of this project: the parameterization of invariant manifolds. It is important to point out that we could not include the proof of the chaotic behavior of the Lorenz attractor, which could be a further investigated to understand strange attractors and complement this paper.

It is also important to take into account the importance of computation in this field. During the development of the work we found that most of the time had to be dedicated to it. We have developed a program written in C code for the numerical integration using Taylor's method, another to compute the Lyapunov exponents and finally a third one to compute the approximation of the parameterization of the invariant stable manifold and the orbit errors. However, the obtained results are worth it and even beautiful. Comparing this work with some other more general ones we realized that working with the specific case of the Lorenz model has really simplified our work.

Finally, we would like to go a little bit further in the parameterization of invariant manifolds and explain how this project could continue. We have achieved an approximation of \mathcal{W}^s of the Lorenz System but it can still be globalized. In [Har10] we can find an introduction of the method of globalization of two dimensional stable or unstable manifolds. This method consists in integrating the normalized Lorenz equations departing from the border of the fundamental domain and adding an extra equation for the derivative of the original time with respect to the arclength. This is done in order to advance the same arclength distance along each trajectory.

References

- [All96] Kathleen T. Alligood, Tim D. Sauer, and James A. Yorke, *Chaos. An introduction to Dynamical Systems* 1st. ed. (Springer-Verlag, New York, 1996).
- [Arg15] J. Argyris, G. Faust, M. Haase and R. Friedrich, *An Exploration of Dynamical Systems and Chaos* 2nd. ed. (Springer-Verlag Berlin Heidelberg, 2015).
- [Bau15] P. Bauer, A. Thorpe and G. Brunet, *The quiet revolution of numerical weather prediction*, (Nature 525, 2015).
- [Bov04] Jo Bovy, *Lyapunov Exponents and Strange Attractors in Discrete and Continuous Dynamical Systems*, (2004).
- [Cab04] Xavier Cabré, Ernest Fontich, Rafael de la Llave, *The parameterization method for invariant manifolds III: overview and applications*, Journal of Differential Equations, (2004).
- [Har10] À. Haro, M. Canadell, J-L. Figueras, A. Luque and JM. Mondelo *The parameterization method for Invariant Manifolds: From Rigorous Results to Effective Computations*, (Springer International Publishing, 2010).
- [Hil00] Robert C. Hilborn *Chaos and Nonlinear Dynamics* 2nd. ed. (Oxford University Press, Oxford, 2000).
- [Jor01] Àngel Jroba and Maorang Zou, *A software package for the numerical integration of ODE by means of high-order Taylor methods*, (2001).
- [Nir10] J.Nirody, *Dynamical Systems Generated by ODEs and Maps*, (2010).
- [Lor60] Edward N. Lorenz, *Energy and numerical weather prediction*, (1960).
- [Lor63] Edward N. Lorenz, *Deterministic Nonperiodic Flow*, (Massachusetts Institute of Technology, 1963).
- [Lor84] Edward N. Lorenz, *Some Aspects of Atmospheric Predictability*, (1984).
- [Pei92] , Heinz-Otto Peitgen, Hartmut Jurgens, Dietmar Saupe *Strange Attractors: The Locus of Chaos*, Chapter 12, (Springer New York, 1992).
- [Tuc02] W. Tucker, *A Rigorous ODE Solver and Smale's 14th Problem*. 53-117, (2002).
- [Wal06] John M. Wallace and Peter V. Hobbs *Atmospheric Science. An Introduction Survey*, 2nd. ed. (University of Washington, 2006).